



Originally published as:

Jin, H., Jin, X., He, R., Luo, D., Chang, X., Wang, S., Marchenko, S. S., Yang, S., Yi, C., Li, S., Harris, S. A. (2019): Evolution of permafrost in China during the last 20 ka. - *Science China Earth Sciences*, 62, 8, pp. 1207—1223.

DOI: <http://doi.org/10.1007/s11430-018-9272-0>

This is a post-peer-review, pre-copyedit version of an article published in Science China Earth Sciences. The final authenticated version is available online at:

<http://dx.doi.org/10.1007/s11430-018-9272-0>

# Evolution of permafrost in China during the last 20 ka

Huijun Jin <sup>1,2,3\*</sup>, Xiaoying Jin <sup>1,3\*</sup>, Ruixia He <sup>1</sup>, Dongliang Luo <sup>1†</sup>, Xiaoli Chang <sup>1,4</sup>, Shaoling Wang <sup>1</sup>,  
Sergey S Marchenko <sup>1,5</sup>, Sizhong Yang <sup>1,6</sup>, Chaolu Yi <sup>7</sup>, Shijie Li <sup>8</sup>, and Stuart A Harris <sup>9</sup>

1. *Northeast China Observational Station of Cold-regions Engineering and Environment, State Key Laboratory of Frozen Soils Engineering, Northwest Institute of Eco-Environment and Resources, Chinese Academy of Sciences, Lanzhou 730000, China;*

2. *School of Civil Engineering, Harbin Institute of Technology, Harbin 150090, China;*

3. *University of Chinese Academy of Science, Beijing 100049, China;*

4. *Hunan University of Science and Technology, Xiangtan, Hunan 411201, China;*

5. *Permafrost Laboratory, Geophysical Institute, University of Alaska Fairbanks, Fairbanks, AK 99775, USA;*

6. *GFZ German Research Centre for Geosciences, Telegrafenberg, D-14473 Potsdam, Germany;*

7. *Institute of Tibetan Plateau Research, Beijing 10010, China;*

8. *Institute of Geochemistry, Chinese Academy of Sciences, 55081 Guiyang, China, and;*

9. *Department of Geography, University of Calgary, Calgary, Alberta, Canada. T2N 1N4.*

\* *Corresponding authors. E-mail: H Jin at [hjijin@lzb.ac.cn](mailto:hjijin@lzb.ac.cn), and X Jin at [lnxyjxy@163.com](mailto:lnxyjxy@163.com)*

† *Author of equal contribution. E-mail: [luodongliang@lzb.ac.cn](mailto:luodongliang@lzb.ac.cn)*

**Abstract:** The formation and evolution of permafrost in China during the last 20 ka were reconstructed on the basis of large amount of paleo-permafrost remains and paleo-periglacial evidence, as well as paleo-glacial landforms, paleo-flora and paleofauna records. The results indicate that, during the local Last Glacial Maximum (LLGM) or local Last Permafrost Maximum (LLPMax), the extent of permafrost of China reached  $5.3 \times 10^6$  km<sup>2</sup>~ $5.4 \times 10^6$  km<sup>2</sup>, or thrice that of today, but permafrost shrank to only  $0.80 \times 10^6$  km<sup>2</sup>~ $0.85 \times 10^6$  km<sup>2</sup>, or 50% that of present, during the local Holocene Megathermal Period (LHMP), or the local Last Permafrost Minimum (LLPMin). On the basis of the dating of periglacial remains and their distributive features, the extent of permafrost in China was delineated for the two periods of LLGM (LLPMax) and LHMP (LLPMin), and the evolution of permafrost in China was divided into seven periods as follows: 1) LLGM in Late Pleistocene (ca. 20,000 ~ 13,000-10,800 a BP) with extensive evidence for the presence of intensive permafrost expansion for outlining its LLPMax extent; 2) A period of dramatically changing climate during the early Holocene (10,800 ~ 8,500-7,000 a BP) when permafrost remained relatively stable but with a general trend of shrinking areal extent; 3) The LHMP in the Mid-Holocene (8,500-7,000 ~ 4,000-3,000 a BP) when permafrost degraded intensively and extensively, and shrank to the LLPMin; 4) Neoglaciation during the late Holocene (4,000-3,000 ~ 1,000 a BP, when permafrost again expanded; 5) Medieval Warming Period (MWP) in the late Holocene (1,000 ~ 500 a BP) when permafrost was in a relative decline; 6) Little Ice Age (LIA) in the late Holocene (500 ~ 100 a BP), when permafrost relatively expanded, and; 7) Recent warming (during the 20<sup>th</sup> century), when permafrost continuously degraded and still is degrading. The paleo-climate, geography and paleopermafrost extents and other features were reconstructed for each of these seven periods.

**Key words:** Permafrost evolution, cryogenic wedge structures, local Last Glacial Maximum (LLGM) (local Last Permafrost Maximum, or LLPMax), local Holocene Megathermal Period (LHMP) (local Last Permafrost Minimum, or LLPMin), China

## 1. Introduction

In China, the local Last Glacial Maximum (LLGM, 26-16 ka BP) was the coldest period and the local Holocene Megathermal Period (LHMP, 8.5-7 ~ 4-3 ka BP) was the warmest period since the end of the Late Pleistocene (Shi, 1998, 2006, 2011; Zheng *et al.*, 1998; Shi *et al.*, 2000). During these two periods, climate fluctuations, in different cold-warm and dry-wet combinations, directly controlled the distribution of glaciers and permafrost and their changes. Therefore, understanding the past and present distribution, degradation rates, shrinking areal extents and volumes of permafrost is key to studying the source and sink effects of climate change and permafrost dynamics on the carbon pools in the atmosphere, soil and shallow permafrost.

49 Although the Last Glaciation Maximum (LGM) was the latest glaciation period, there was no a uni-  
50 fied ice sheet, and snow and ice coverage was limited on the Qinghai-Tibet Plateau (QTP) and its periph-  
51 eral mountains (Shi *et al.*, 1990, 1995; Zheng, 1990; Shi, 2006, 2011; Heyman, 2010). Permafrost may  
52 have intensively developed, extensively expanded and reached the local Last Permafrost Maximum  
53 (LLPMax), establishing the framework of existing permafrost in China (Zhao *et al.*, 2013). Later, it under-  
54 went the local Last Permafrost Minimum (LLPMin) in the local Holocene Megathermal Period (LHMP)  
55 and a series of evolutionary processes, forming the present distributive features of permafrost in China  
56 (Zhou *et al.*, 1991; Qiu and Cheng, 1995; Zhou *et al.*, 2000; Jin *et al.*, 2007a, 2016; Chang *et al.*, 2017).

57 At present, the areal extent of permafrost in China is  $1.59 \times 10^6$  km<sup>2</sup>, including an areal extent of plat-  
58 eau permafrost at  $1.05 \times 10^6$  km<sup>2</sup> on the QTP, an areal extent of latitudinal permafrost at  $0.24 \times 10^6$  km<sup>2</sup> in  
59 Northeast China, an areal extent of mountain permafrost at  $0.30 \times 10^6$  km<sup>2</sup> mainly in West and Central  
60 China (Ran *et al.*, 2012). The areal extent of seasonally frozen ground in China at present is  $5.36 \times 10^6$  km<sup>2</sup>,  
61 mainly found in North and Central China. In addition, at the beginning of the last 20 ka, permafrost may  
62 have occurred in most regions in Northwest, North, and Northeast China and on the Qinghai-Tibet Plateau.  
63 Rising sea levels permitted the East Asian Monsoon to re-develop, resulting in a change from very cold,  
64 dry conditions to warmer, more humid conditions marked by the rise and decline of ice-wedges, leaving  
65 behind a large amount of evidence and landscapes of Quaternary permafrost and periglacial phenomena. In  
66 this paper, the evolution processes and distributive features of permafrost in China since the last 20 ka  
67 were reconstructed on the basis of clarifying and using those numerous reported and recently identified  
68 evidence and proxies for inferring the past permafrost and periglacial environment. This study aims at  
69 providing a basic understanding and key scientific baseline for rebuilding the cold regions environment  
70 and carbon turnovers and their change rates among the glacial and interglacial periods in China and be-  
71 yond.

## 72 2. Study Methods

### 73 2.1 Research method for Quaternary paleo-permafrost

74 Under the dry cold conditions at ca. 20-21 ka BP ( $21 \pm 2$  ka BP), there was negligible water supply so that  
75 ice-wedges could not form. With the onset of the East Asian Monsoon due to rising sea levels, the warm  
76 precipitation entered the soil, producing ice wedges and bodies of ice. The heat, brought with the precipita-  
77 tion, plus the heat emitted during crystallization, resulted in warming the surrounding permafrost. The re-  
78 sulting ground ice is the evidence for past permafrost and paleo-periglacial geomorphology. However,  
79 their evidence is often subject to various interpretations (e.g., Vandenberghe, 1992; Vandenberghe and Pis-  
80 sart, 1993; Murton and Kolstrup, 2003; Harris *et al.*, 2017; French, 2018). The formation, development,  
81 areal extent and evolution of past permafrost are estimated and reconstructed on the basis of Quaternary  
82 geology and paleo-biology, -climatology and -environmental proxies and data, and related dating tech-  
83 niques, under the principle of “the present as the key to the past”, often aided by numerical model recon-  
84 struction (e.g., Liu *et al.*, 2002; Jiao *et al.*, 2015, 2016).

### 85 2.2 Evidence and criteria for past permafrost

86 The evidence for the occurrence of permafrost can be classified into two categories: direct and indirect in-  
87 dicators. Direct indicators include primary and secondary wedge structures, deeply buried permafrost and  
88 massive ground ice, past permafrost tables, pingos and pingo scars, lithalsas and palsas, to just name a few.  
89 Indirect indicators can be cryoturbations or cryogenic involutions, soil wedges and cryogenic polygonal  
90 structures, active or paleo-rock glaciers (e.g., Schmid *et al.*, 2015); sorted and patterned ground, block  
91 fields, as well as pollen records in soil strata, such as *Picea* and *Abies* or other indicators of cold floristic  
92 communities, paleosols; glacial tills and landforms; periglacial flora and fauna (such as mammoths, woolly  
93 rhinos, and hardy plants), and characteristic combinations of clay minerals in soil strata. Some of these in-  
94 dicators are subject to multifaceted interpretations. Reliable conclusions can only be reached by compre-  
95 hensive studies using multi-proxy combinations and cross-examinations.

96 The response of permafrost to climate change has a substantial time lag. On the ground surface, the  
97 relics of previous permafrost stages are often buried or erased by the next or new evolution events, only to

98 increase the challenges for reconstructing a more detailed sequence of permafrost evolution. In another  
99 word, the closer to the present, the richer and more detailed the identified relics of permafrost. Therefore,  
100 various permafrost relics since the last 20 ka have been relatively better preserved. In recent decades, con-  
101 tinuous and rapid advancement in sediment dating, more sophisticated and accurate dating methods, and  
102 continuous enrichment of various experimental and geoscience data have enabled more systematic ap-  
103 proach and methods, and have resulted in more reliable results. In order to draw better conclusions in the  
104 formation and development of the permafrost environment, it is necessary to combine and validate with  
105 the results from Quaternary glaciology, desert research, periglacial studies, and paleo-climatology, -geog-  
106 raphy and -environment. These processes can largely overcome the multiplicity in the interpretations for  
107 some periglacial phenomena and eliminate as possible the false understanding.

108 The estimation of paleo-ground-temperature is important in understanding the occurrence and  
109 developmental conditions of past permafrost. It can be achieved by using the paleo-air-temperatures, or  
110 interpretations from various paleo-cryogenic wedge structures. On the basis of field observations and lab  
111 experiments, [H. H. Романовский \(1977\)](#) summarized and pointed out that cryogenic wedge structures, such  
112 as soil/ground, sand and ice wedges, as well as ice-wedge pseudomorphs (casts), as a result of cryogenic  
113 polygonal cracking, were closely related to the properties of soil sediments, soil moisture contents, and  
114 ground temperatures. The finer the soil grains, the lower the temperatures for the formation of cryogenic  
115 wedge structures. To grow soil wedges in fine-grained soils, such as fine sands, silts, sandy loams, clay, peat  
116 and humic soils, a mean annual ground temperature (MAGT) of  $-2 \sim -1$  °C, or lower, is needed, whereas  
117 those in the coarse-grained soils, such as medium and coarse sands and sandy gravels, would need an MAGT  
118 of  $-5 \sim -3$  °C, or lower, while ice wedges in coarse soils would mandate an MAGT of  $-6 \sim -5$ °C or lower.  
119 Up to date, this method of using cryogenic wedge structures for inferring paleo-temperatures have been  
120 widely adopted as a traditional method in rebuilding the Quaternary permafrost environment in China (*e.g.*,  
121 [Cui, 1980](#); [Liang and Cheng, 1984](#); [Pan and Chen, 1997](#); [Cui et al., 2002, 2004](#); [Jin et al., 2007a, 2011a,](#)  
122 [2011b, 2016](#); [Chang et al., 2011, 2017](#)), and beyond (*e.g.*, [Harris et al., 2017](#); [French, 2018](#)).

### 123 **3. Statistics on paleo-permafrost and criteria for southern/lower limit of permafrost**

#### 124 **3.1 Statistics on paleo-permafrost**

125 The ages for the formation and thawing of paleo-permafrost are key in statistics and analyses of various  
126 paleo-permafrost relics and data. The authors of this paper have extensively collected, varified and extended  
127 the dating data on the basis of Quaternary glacial periods in China provided by [Shi \(2006\)](#), in addition to the  
128 statistics of related age data for past permafrost in China ([see Supplementary materials](#)). These data serve as  
129 the baseline for the divisions of chronological sequences of permafrost evolution in China. They were further  
130 elaborated with several representative profiles of wedge structures and some photos of typical cryogenic  
131 structures ([Figure 1](#)).



132  
133 a) Ice wedges in Wuma, northern Da Xing'anling Mts.



134  
135 b) Cryoturbations in Dishaogou Valley, Salawusu, Inner  
136 Mongolia. cryoturbations in yellowish fine sand with  
137 grayish silts



138  
139 c) Sand wedges in Huang'he Village, Madoi, Qinghai



140  
141 d) Pingo scars northwest of the Ngöring Lake, SAYR



142  
143 e) Cryoturbations on the first terrace of the Datong River  
144 near Huangchengzi, Menyuan, Qinghai: 150×5 m, loca-  
145 tion at 37°38'25.2"N, 101°9'43.3"E; 3,148 m asl



146  
147 f) Frost-cracking sand wedges at Yixing Logistics Co. in  
148 Dongsheng, Ordos, Inner Mongolia

149 **Figure 1. Photos of typical cryogenic structures in China (only 6 sites are listed)**

### 150 3.2 Delineation of paleo-permafrost boundaries

151 Paleo-permafrost remains, e.g., ice wedge pseudomorphs (casts) and rock, sand, soil and primary ice  
152 wedges in particular, are key indicators for rebuilding the paleo-environment and Quaternary boundaries of  
153 permafrost. Large numbers of wedge structures with various shapes and geneses have been identified. They  
154 can only be indicative of paleo-permafrost when they are clarified and verified as groups of cryogenic sand,  
155 soil and rock wedges closely related to frost cracking polygons and permafrost. By using the relationships  
156 of wedges to the host strata, ice wedges and ice wedge pseudomorphs (casts), and sand, soil and rock wedges  
157 can be recognized. Ground temperatures for the formation of wedge structures are related to wedge structure  
158 types and soil strata. Due to rapid tectonic uplifts in recent geohistory, it is necessary to make elevational  
159 and latitudinal adjustments for estimated air or ground temperatures: 6°C/km (elevation) and 1°C/°N (Zhou  
160 *et al.*, 2000).

161 Since the Late Peistocene, the QTP has been uplifted by about 1,000 m. Due the short time period  
162 involved in this discussion, an elevation of 500 m, as justified in Zhou (2007), is assumed in this paper. In  
163 addition, the adjustments have to take into account the tectonic units of these identified cryogenic structures,  
164 such as those of the Tianshui'hai Lake region in the relative uplift zone in the West Kunlun Mountains, and  
165 Nachitai along the Qinghai-Tibet Highway (QTH) in the Eastern Kunlun Mountains, the Gong'he Basin on  
166 northeastern QTP, and the Lenghu Basin on northern QTP in the relative subsidence zone. The  
167 southern/lower limit of permafrost (SLP/LLP) and distributive features, as well as paleo-geography, can  
168 then be delineated on the basis of adjusted air or ground temperatures.

#### 4. Results and discussions

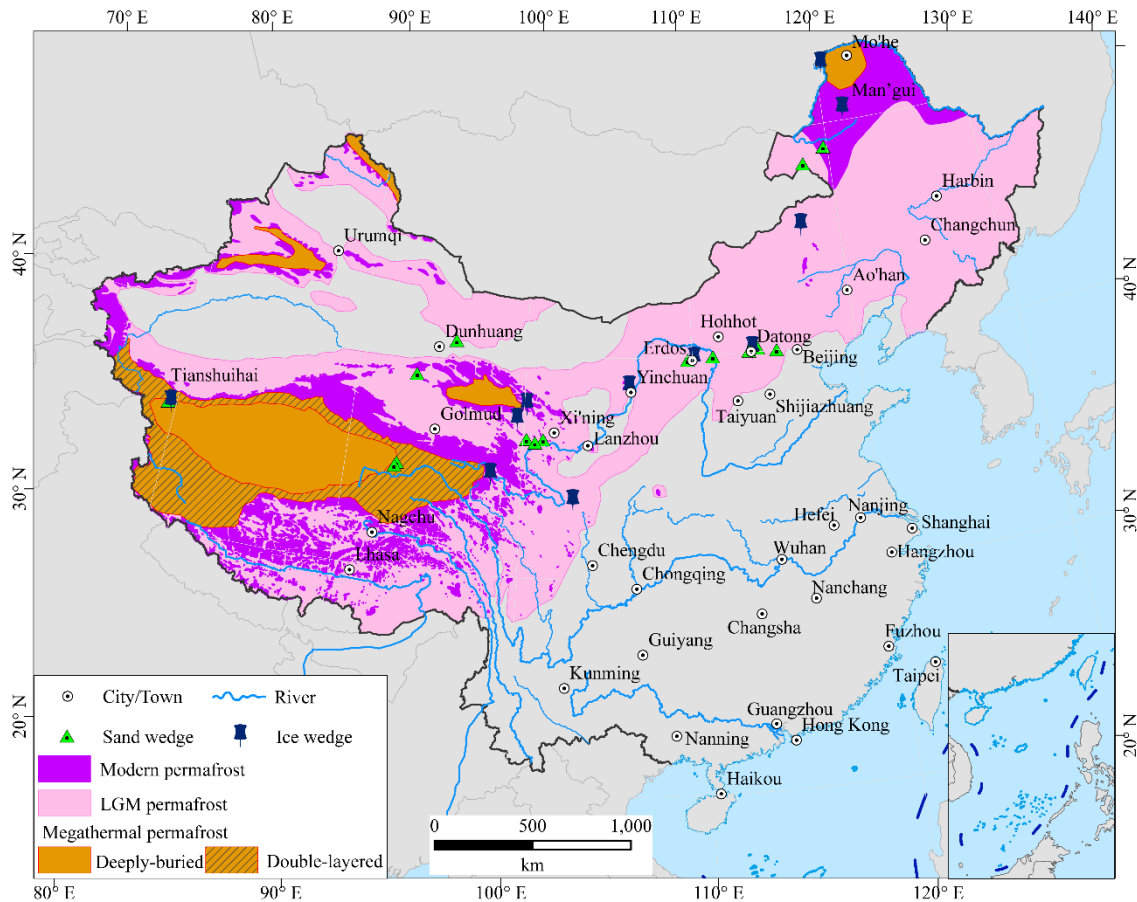
170 Many paleo-permafrost and paleo-periglacial remains of different ages since the Middle Pleistocene  
171 have been identified in China (*e.g.*, Pan and Chen, 1997; Zhou *et al.*, 2008; Qi *et al.*, 2014). However, the  
172 main body of the existing permafrost in China was formed during the LLGM in the Late Pleistocene (Zhou  
173 *et al.*, 1965, 2000; Zhao *et al.*, 2013; Jin *et al.*, 2016; Chang *et al.*, 2017). Since the Late Glacial period in  
174 the early Holocene, permafrost has undergone many expansions and retreats, forming the present distributive  
175 patterns of permafrost in China.

176 Taking into account of lagged responses of permafrost to climate changes, the LLPMax occurred about  
177 20 ka BP (ca. 21±2 ka BP). Later, many major climatic and environmental changes, such as the LLGM and  
178 LHMP, have reshaped the distributive features of permafrost (Zheng *et al.*, 1998). The LLPMax and LLPMin  
179 in China also took place (Figure 2) (Zhao *et al.*, 2013; Harris *et al.*, 2016; Jin *et al.*, 2016; Chang *et al.*,  
180 2017).

181 Permafrost evolution in China since 20 ka BP can provisionally be divided into seven major periods on  
182 the basis of the distribution of existing permafrost in China and analyses of spatiotemporal differentiations  
183 of paleo-permafrost and -periglacial remains listed in the Supplementary materials, in addition to cross-  
184 correlations with Quaternary glacial, paleo-climatic and -environmental records. Among them, the  
185 LLGM/LLPMax and LHMP/LLPMin are the most important periods for the development, growth and  
186 evolution, as well as the distribution, of the existing permafrost in China. In those above-mentioned seven  
187 periods, some sub-tier changes in climate, permafrost and periglacial environments occurred. However, the  
188 responses of permafrost to these second-tier changes have been overlapped or erased by these seven major  
189 climate climaxes (the coldest or warmest). Therefore, under these complex circumstances, only distribution  
190 of permafrost under those longer-term climate extremes, *i.e.*, the maxima or minima of permafrost extent,  
191 can be rebuilt.

192 On the studies and integration of paleo-permafrost in the periphery or bordering states and/or regions, an  
193 attempt is made for merging the reconstruction of LLGM permafrost in China with some other regions  
194 (Figure 2). It seems that the boundaries of permafrost in China merge with those in Kazakhstan, Central  
195 Asian states, and western Asia. However, it still needs data from Russia, Mongolia and Korean Peninsula to  
196 integrate the paleo-permafrost map with Eurasian permafrost body during the LLGM. In the meantime, it  
197 should be pointed out that due to large amplitudes of sea level drop as much as 120-150 m during the this  
198 LLGM, the general circulations and distribution of land-ocean, as well as some major landscapes and  
199 vegetation, were affected, complicating the reconstruction of paleo-permafrost in China and bordering states.  
200 In particular, these mosaicked distributions of permafrost and talik in deserts have been discussed, but still  
201 lack reliable evidence for mapping these regions.





202

203

Figure 2. Distribution of permafrost in China during the LLPMax/LLGM, LLPMin/LHMP, and at present

204

**4.1 Permafrost expansion during the LLPMax in the end of the Late Pleistocene (LLGM , ~20 to 13~10.8 ka BP): permafrost was extremely well developed and intensively expanded**

205

206

207

208

209

210

211

212

213

214

215

216

217

218

219

220

221

222

The climax of LGM (26~16 ka BP) witnessed the latest large-scale glaciations, with a massive cooling in the Northern Hemisphere (Shi, 1998; Shi *et al.*, 1990, 1995, 1997; Zheng, 1990; Wang and Sun, 1994; Zheng *et al.*, 1998). In the meantime, glaciations expanded in North China and on the QTP; however, the spatial scales of glaciations were limited on the QTP and in its periphery mountains, and mountains in Central Asia, and Northeast, North and Central China (Sun *et al.*, 1985; Li *et al.*, 1991; Shi *et al.*, 2000; Shi, 2006; Heyman, 2010). Therefore, it could have been the LLPMin in China. Many paleo-permafrost and -periglacial remains have been well and extensively preserved (Supplementary materials). In particular, large numbers of cryogenic wedge structures, especially those extensively identified sand and soil wedge groups, formed during the LLGM, have been found in China. In addition, numerous cryogenic wedge structures have also been discovered and archived in most regions of what is seasonally frozen ground at present, such as the Ordos (Loess) Plateau, QTP, North China and southern part of Northeast China (*e.g.*, Zhang, 1983; Xu and Pan, 1990; Wang and Bian, 1993; Pan and Chen, 1997; Cui *et al.*, 2004, 2004; Vandenberghe *et al.*, 2004, 2016; Cheng *et al.*, 2006; Jin *et al.*, 2006a, 2006b, 2007a, 2016; Zhou, 2007; Zhou *et al.*, 2008; Chang *et al.*, 2011, 2017; Harris and Jin, 2012; Wang *et al.*, 2013; Xu *et al.*, 2015; Harris *et al.*, 2016, 2018). These wedges were generally formed at the margins of lacustrine or river terraces, and covered by sediments of 1~2 m thicknesses. In profiles of some of those wedge structures, falling textures and blocky and gravelly infills can be identified, which can be related to the melting of ground ice.

223 A very cold and dry climate prevailed on the QTP during the LLGM until 14 ka BP. Afterwards, climate  
224 warmed up intermittently, and the growth of some wedges stopped due to the rising air temperatures.  
225 According to the ice-core records from the Guliya Ice Cap in the West Kunlun Mountains, a warming of  
226 about 2~3°C occurred during 14~12 ka BP, although there were still appreciable ups and downs in air  
227 temperatures (Shi, 2011). By the end of the Late Peistocene, the major distributive patterns of existing  
228 permafrost on the QTP were already established (Jin *et al.*, 2007a; Chang *et al.*, 2017).

229 On the basis of the interpretations for numerous wedge structures, there was a cooling of about 7~9°C on  
230 the QTP at ca. 20 ka BP (Jin *et al.*, 2007a; Chang *et al.*, 2017). Shi *et al.* (1995, 2000) concluded that, on  
231 middle and eastern QTP, it was 6.8°C colder than today. On the Zoigé Peat Plateau, a cooling of 5.8~7.9°C  
232 occurred, as inferred from an 1,200-m lowering of the upper timberline. Based on pollen records, the  
233 deduced paleotemperatures at the LLGM were about 6~7°C cold than today (Shen *et al.*, 1996). On the basis  
234 of paleo-periglacial landforms, Cui (1980) estimated a cooling of 5.5~6.4°C for the Tanggula Mountains in  
235 the Interior of the QTP. By comparing the changes in the lower limits of paleo-permafrost, Yang and Wang  
236 (1983) estimated a cooling of 5~6°C for the plateau regions south of the Tanggula Mountains. Zheng (1990)  
237 believed that because of the large areal extent and massive relief of the QTP, there should be a marked  
238 differentiation in climate cooling during the LLGM: a cooling of 5~7°C in the Interior and alpine regions of  
239 the QTP, but the cooling could be as much as 8~10°C in the peripheries. On the basis of surface pollen  
240 records in Rencuo, Basu County, Tibet Autonomous Region, Tang *et al.* (1998) deduced that the mean  
241 January air temperature at ca. 18 ka BP was 10°C lower than today, *i.e.* a cooling of about 6°C. On the basis  
242 of large cryoturbations and glaciofluvial sediments in Menyuan, Qinghai Province, Wang *et al.* (2013)  
243 estimated an LLGM cooling of at least 7°C, resulting in glaciers advancing to the foothills of the Qilian  
244 Mountains. Vandenbergh *et al.* (2016) and Harris *et al.* (2016) also have similar notions.

245 Numerical climate model reconstruction on the QTP indicate an LLGM cooling of 2~13°C (Liu *et al.*,  
246 2002), 6°C (Böhner and Lehmkühl, 2005), and 1.8~6.4°C (Ju *et al.*, 2007). Mark *et al.* (2005) estimated an  
247 LLGM cooling of 7.5°C on the QTP according the changes in snowline, or the equilibrium line altitude  
248 (ELA). In a word, most scholars more or less have reached similar conclusions on the LLGM magnitude of  
249 the cooling on the QTP. Thus, it is reasonable to assume an LLGM cooling of 7~9°C. However, Heyman  
250 (2010) and Owen *et al.* (2003, 2006) suggested that the glacial expansion was very limited on the basis of  
251 their latest studies on the QTP and adjacent regions with an LLGM of cooling (2~4°C). There was no unified  
252 QTP or regional icesheet; most of plateau glaciers were formed long time ago and with only limited  
253 expansions during the LLGM (Heyman *et al.*, 2008, 2009; Stroeven *et al.*, 2009).

254 Groups of inactive ice wedges were also found in Wuma (52°45'N, 120°45'E), northwestern corner of  
255 the Da Xing'anling Mountains, Northeast China (Tong, 1993). On the basis of AMS-<sup>14</sup>C dating of ambient  
256 and overburden soils of the ice wedges, they were formed during 14,475±304~10,668±257 a BP. It would  
257 need a mean annual air temperature (MAAT) of about -7 ~ -5°C for forming ice wedges in the sandy soils  
258 (Nomanovskii, 1977). The observations indicate that the present MAGT is 3.8~4.3°C higher than the MAAT  
259 in the northern Da Xing'anling Mountains (Chang *et al.*, 2015; Jin *et al.*, 2016). Therefore, it is estimated  
260 that, when these ice wedges were formed, the local paleo-MAAT was about -10 ~ -9°C (Tong, 1993). The  
261 present-day MAAT in this region was about -5°C (in the 1990s). Therefore, the northern Da Xing'anling  
262 Mountains was about 4~5°C colder during the ice wedge growth period than today (Jin *et al.*, 2016). To the  
263 south in the middle-western part of Northeast China, the Hulun Buir High Plain was sparsely vegetated  
264 under a dry continental climate during 22~11 ka BP (Yang *et al.*, 2006).

265 In the arid regions in North China, Yu *et al.* (2013) rebuilt the paleoclimate during the LLGM (ca.  
266 26~16 ka BP) on the basis of a large amount of paleodata, with a climate cooling of about 5~11°C and a  
267 variability (uncertainty) of 60%~200%; the concurrent decline in annual precipitation was about 180~350  
268 mm. In the end of the Late Pleistocene, the present-day topography, geomorphology and topography were  
269 largely formed in the arid regions in Northeast and North China. Therefore, the SLP at the LLGM can be  
270 largely determined by the 0°C isotherms of MAAT (Jin *et al.*, 2007b). In Northeast China, assuming an  
271 MAAT of 4~5°C colder than today and a northward cooling rate of 1°C/°N (Zhou *et al.*, 2000), the SLP at



272 the LLGM could have extended southwards by 4°~5°N, *i.e.*, reaching 41°~42°N (Figure 2). The LLGM SLP  
273 and LLP met in the Liupanshan and Hua'jialing mountains on the Longdong Plateau (near Lanzhou) at  
274 elevations of 2,200-2,300 m asl (Zhou *et al.*, 2000; Jin *et al.*, 2007a, 2016; Zhao *et al.*, 2013; Chang *et al.*,  
275 2017). This estimation was later confirmed by discoveries of many frost-cracking wedges on the Ordos  
276 (Loess) Plateau and reconstructed the latest coldest paleoenvironment in the LLGM of about 10~12°C colder  
277 than today during 25~13 ka BP, when permafrost expanded southwards to south of 37°~38°N (Cui *et al.*,  
278 2004; Vandenberghe *et al.*, 2004).

279 On the QTP and in alpine regions in Central and West China, the MMAT at the LLP generally ranges  
280 from -4 ~ -2°C. There the LLP decreases by about 160-170 m for every 1°C cooling in MAAT (Wang and  
281 Bian, 1993). The LLP during the LLGM was 1,200-1,400 m lower than that of today, inferred from the  
282 combined evidence from the 7~9°C cooling of MAAT on the QTP and in alpine regions, the distribution of  
283 cryogenic wedge structures and other periglacial remains, and the lowering of the upper timberline (Jin *et*  
284 *al.*, 2007a; Zhao *et al.*, 2013; Chang *et al.*, 2017). The plateau permafrost expanded and descended into the  
285 periphery inland basins, such as Xinghai, Gong'he, Zoigé, Chaidam and Tarim basins, with an areal extent  
286 of continuous permafrost at about 2.2×10<sup>6</sup> km<sup>2</sup>. Sporadic and isolated patches of permafrost were also  
287 extensively distributed in mountainous areas in West China. Thus, the LLP could be estimated as follows:

288 1) On western and northwestern QTP, the LLP was at 2,800-2,900 m asl in western section of northern  
289 slopes of the West Kunlun Mountains, at 2,400-2,500 m asl on eastern section of northern slopes of the West  
290 Kunlun Mountains, and at 2,900-3,100 m asl in the southern margin of the Tarim Basin;

291 2) On eastern QTP, the LLP was at 2,300-2,400 m asl in the Gong'he Basin, 2,600-2,800 m asl in the  
292 Chaidam Basin, 2,700-2,800 m asl on the Zoigé Plateau, 3,000-3,200 m asl on the Chuanxi (West Sichuan)  
293 Plateau, and 3,800-4,000 m asl in the Hengduan Mountains; on southern QTP, it was at 3,600-3,800 m asl  
294 in the middle- and down-streams of the Yarlong Zangpo River Basin in southern Tibet Autonomous Region;

295 3) On northern QTP, the LLP was at 2,200-2,300 m asl on northern slopes (Lenglongling Mountains) of  
296 Qilian Mountains and mountainous regions south of the Jiayuguan Pass, Gansu Province and;

297 4) The LLP was at 2,100-2,200 m asl on southern slopes and at 1,900-2,000 m asl on northern slopes of  
298 the Chinese Tianshan Mountains, and 1,400-1,500 m asl on southern slopes of the Chinese Altai Mountains.

299 In summary, except for taliks in some deserts and lowland basins, the majority parts of North China  
300 and QTP were in permafrost zones (Figure 2), with a total permafrost extent at 5.3×10<sup>6</sup>~5.4×10<sup>6</sup> km<sup>2</sup>, or  
301 three times of the present permafrost extent.

302 During the LLGM, periglacial landforms were extensively developed, leaving behind many relics, such  
303 as those primary sand wedges in medium and fine sands (Q<sub>3</sub> Gong'he Group sediments) on northeastern  
304 QTP reported by Xu (1984), Pan and Chen (1997), with a formation time prior to 20,403±430~19,430±360  
305 a BP. Numerous sand wedges and ice wedge pseudomorphs have been identified and studied in the Source  
306 Area of the Yellow River with a formation age at 12,300±100~16,340±250 a BP (Pan and Chen, 1997;  
307 Cheng *et al.*, 2006). The soil wedges in Nachitai on northern slopes of the Kunlun Mountains along the QTH  
308 were formed during 14,041±339~15,377±292 a BP; those sand wedges in the Fenghuoshan Mountains in  
309 the Interior of the QTP were formed at 23,500±1200 and 15,340±770 ~9,218±189 a BP. Sand wedges in  
310 Lenghu of the middle and northern parts of Qinghai Province were TL-dated at 18,510±2,220 a BP (Ma,  
311 1996). Inactive ice wedges and primary sand wedges on the terrace of the Tianshuihai North Lake in the  
312 West Kunlun Mountains were formed during 21-12 ka BP (Li and He, 1990; Li and Jiao, 1990; Chang *et al.*,  
313 2011). In a 5-m-high roadcut close to Huangchengzi, Menyuan Hui Prefecture, Qinghai Province, on the  
314 southern flank of the Qilian Mountains, very large load castings developed during the OSL 20~30 ka BP  
315 (Vandenberghe *et al.*, 2016; Harris *et al.*, 2016).

316 Due to the extremely cold and dry continental climate, the plateau vegetation severely degraded during  
317 the LLGM. The majority of the plateau surface reverted to desert, steppe, or tundra environments: lakes  
318 shrank and deserts expanded. Steppes extended eastwards to Linxia, Gansu Province and to the Zoigé Plateau,

319 Sichuan Province, and southwards to Basu County to the Yarlung Zangpo River Basin, southeastern Tibet  
320 Autonomous Region. Forests retreated to the eastern and southern edges of the QTP, with only some small  
321 patches of alpine shrublands and mountain needle- and broad-leaved mixed forests on the Western Sichuan  
322 and south of the Yarlung Zangpo River (Tang *et al.*, 1998).

323 In Northeast China, a rich pollen assemblage of *Picea* and *Abies* have been found in the strata of the  
324 Guxiangtun Group in the Late Pleistocene in Huangshan, Harbin, Heilongjiang Province and Yushu County,  
325 Jilin Province, indicating for a forest-steppe landscape. Based on incomplete statistics, fossils and remains  
326 of Mammoths (*Mammuthus*)-wooly Rhino (*Coelodonta*) fauna, an indicator for cold climate, have been  
327 excavated in many places in southern part of Northeast China and in the northern part of North China,  
328 concentrated in areas north of 42°N (Qiu, 1985; Zhang, 2009; Wei *et al.*, 2010). By integrating the evidence  
329 from the extensive occurrences of the dark needle-leaved forests and Mammoths (*Mammuthus*)-wooly Rhino  
330 (*Coelodonta*) fauna in these regions, it is evident that in the end of the Late Pleistocene, cold climate  
331 prevailed in northern and mountainous parts of Northeast China, as well as the Songhuajiang-Liao'he Plain  
332 in Northeast China (Guo and Li, 1981), even in the lately exposed extensive continental shelves as a result  
333 of lowering sea level (Zhao *et al.*, 2013; Jin *et al.*, 2016). Since the 1970s, many megafauna, such as  
334 *Mogaloceros ordosianus* and *Mammuthus*, have been excavated in primary strata of the Late Pleistocene in  
335 the Bay of Bo'hai Sea. This at least can serve as concrete evidence for cold climate in Northeast China.

336 Since coming into the Holocene, in comparison with the LLPMax/LLGM, the areal extent of permafrost  
337 was on a general decline. The history of permafrost evolution can still be divided into six distinct periods  
338 since the early Holocene starting at 10.8 ka BP.

#### 339 **4.2 Early Holocene with dramatic climate changes (10,800 a BP to 8,500~7,000 a BP): period of stable** 340 **but relatively shrinking permafrost**

341 The climate in the early Holocene was very unstable. A sharp cooling is indicated by the ice-core records  
342 from the Dunde Glacier, Qilian Mountains (38°06'N, 96°24'E; 5,200 m asl): at 8,700 a BP,  $\delta^{18}\text{O}$  reached  
343  $-12.75\%$ , the lowest in the Holocene, whereas  $-9.60\%$  at 8,500~8,400 a BP, the highest in the Holocene,  
344 indicating a spike in climate warming (Yao and Shi, 1992). Accordingly, the diatom records in the Angren  
345 Co (Lake) in southern Tibet Autonomous Region indicate a lower lake temperature and a rising lake water  
346 salinity, *i.e.*, a cold and dry period, prior to 8,700 a BP (AMS- $^{14}\text{C}$ ), but during 8,700~8,600 a BP, the records  
347 suggest a very high lake temperature, with lowered lake water salinity and large input of glacier-melt (Li  
348 and Jiao, 1990).

349 The climate in early Holocene was cold and dry, but it was gradually changing to cool and moist climate.  
350 On the basis of remains of paleo-permafrost, the northern LLP was at 3,400~3,500 m asl to the north of  
351 Nachitai along the QTH, the southern LLP was at 4,200~4,300 m asl between Yangjiajing and Damxung,  
352 northern Tibet Autonomous Region; the LLP then was about 600~700 m lower than today. Permafrost was  
353 continuous and thermally stable, but overall it was degrading from the LLPMax, with a declining areal extent  
354 of permafrost, but the permafrost extent was still 40%~50% greater than today.

355 Song and Xia (1990) reported 150 pingo scars on the Sanjiang Plain (47°10'~48°43'N, 133°~135°E) in  
356 the northern part of Northeast China. They are generally accompanied by pingo-thawed lakes in round or  
357 oblong shapes, with a diameter of about 10~100 m. The outer margins of pingo scars generally have a wall  
358 of about 23 m in height, with an outlet. Generally, inside the walled lakes, water bodies can be found, or  
359 they have gradually developed into wetlands. Most of these pingo scars were formed during 10~8 ka BP (Li,  
360 1990; Song and Xia, 1990). Therefore, it is evident that permafrost still occurred on the Sanjiang Plain in  
361 the early Holocene, but permafrost to the south had largely vanished.

362 On the basis of pollen records from 20 lakes on the QTP, Tang and Shen (1996) synthesized the  
363 environmental features of the plateau in the early Holocene as follows. During ca. 10,000~9,100 a BP,  
364 meophytic deciduous broad-leaved and needle-leaved forests dominated on eastern QTP; during ca.  
365 10,800~8,000 a BP, *Artemisia* and *Chenopodiaceae* dominated in the subalpine steppe in the region of the  
366 Qinghai Lake on northeastern QTP, in which at 9,500~8,800 a BP, there was an evident spike of arbor

367 species pollens of more than 50%, indicating a sudden warming and wetting (Du *et al.*, 1989). During  
368 10,000~7,700 a BP, *Artemisia* dominated steppes on the western QTP under a cold and moist climate.

369 In summary, the plateau climate was wetting and warming, forming wetlands in basins and valleys and  
370 depositing peat and thick layers of humus. For example, the thick-layered peat at the bottom of soil profiles  
371 in Wumaqú, Damxung and Qinongga, Yangbajing, in the Tibet Autonomous Region is AMS-<sup>14</sup>C-dated at  
372 8,175±200~9,970±135 a BP, indicating a starting period of peat formation (Li, 1982). For another example,  
373 dark silty sand clay is found at depths of 2.5~3.0 m in the Borehole CK80 at Qingshui'he Riverside along  
374 the QTH. A soil sample at depths of 2.7~3.0 m is dated at 8,800±305 a BP. Meanwhile, the lithology changes  
375 upward from yellow sand clay and medium-fine sand with limestone blocks and carbonate nodules at the  
376 bottom to dark silty sand clay deposits at the upper part. This transition is a result of climate warming and  
377 wetting and subsequent enrichment of organic matter. In addition, humic silt and sand at the upper part of  
378 sand wedges on the second terrace of the Zuomoxikong Qǔ (River) in the Fenghuoshan Mountains along  
379 the QTH is dated at 9,218±189 a BP, while that at the Highway Maintenance Squad Station (HMSS) 82  
380 along the QTH at the southern piedmont of the Fenghuoshan Mountains was dated at 9,160±170 a BP. They  
381 all indicate an ameliorating climate and no growth of frost cracks and sand wedges. Warming climate was  
382 conducive to plant growth; as a result, some sand dunes formed during the end of the Late Pleistocene were  
383 (semi)fixed. For example, buried plant roots and stems in the sand ridges 2 km southeast of Wudaoliang  
384 along the QTH is <sup>14</sup>C-dated at 9,716±270 a BP (Wang, 1989).

### 385 **4.3 Local Holocene Megathermal Period (LHMP) (8,500~7,000 to 4,000~3,000 a BP: intensive** 386 **permafrost degradation**

387 The mid-Holocene is the optimal climate period in the Holocene, so it is also called the hypsithermal  
388 period, or LHMP. According to Shi *et al.* (1992), the LHMP in China occurred during 8,500-3000 a BP,  
389 with a stable warm and wet climax at 7,200~6,000 a. During the LHMP, it was 1~2°C warmer than today  
390 in South China and in the middle- and down-streams of the Yangtze River Basin, 3°C warmer than today  
391 in North, Northeast and West China, 4~5°C warmer than today on the QTP in Southwest China, and the  
392 warming in winter was much more pronounced. For example, in the ice-core record from Gulia Ice Cap,  
393 at the climax of the LHMP,  $\delta^{18}\text{O}$  was 3‰ higher than the average of the  $\delta^{18}\text{O}$  during the last millenium,  
394 *i.e.*, a warming of about 4~5°C (Shi, 2006). The climate warming in the arid regions in North China could  
395 have been about 1.0~3.5°C in MAAT (with an uncertainty of 20%~130%); annual precipitation increased  
396 by 30~400 mm (with an uncertainty of 10%~120%). The increase in annual precipitation also had a trend  
397 of inland increasing from Southeast China to Northwest China (Yu *et al.*, 2013).

398 The field surveys indicate that the ice wedges in Wuma in northern part of the Da Xing'anling  
399 Mountains were formed during the LLGM and were preserved well before the last inspection in 2007. There  
400 were thawed concaves on the top 0.7 m of the ice wedges, an evidence for the lowering permafrost table.  
401 This implies that in spite of a warming climate during the LHMP, the periglacial environment still prevailed  
402 in the area (Tong, 1993; Jin *et al.*, 2016). In addition, in the Amu'er in northern part of the Da Xing'anling  
403 Mountains (52°51'N, 123°11'E), analysis on the light and heavy mineral contents of Quaternary deposits  
404 indicate low contents of unstable and relatively stable minerals, and even less stable minerals (<5%); in  
405 contrast to 75%~92% in the gravels (Guo *et al.*, 1981). This also indirectly demonstrates that the northern  
406 part of the Da Xing'anling Mountains have never undergone a long-term warm and wet climate. The above-  
407 mentioned two areas are now still in the continuous permafrost zone.

408 With rising temperature in the LHMP, permafrost in China retreated extensively, and latitudinal  
409 permafrost **disappeared from** eastern Inner Mongolia, eastern Xinjiang, and North China. Most latitudinal  
410 permafrost in Northeast China also disappeared, or retreated to the northwestern corner (north of Amu'er-  
411 Mangui) of the Da Xing'anling Mountains to the north of 51°~52°N (Figure 2). Because of the northward  
412 retreat of the SLP by 3~4°N, the climate warming could be about 3~4°C warmer than today.

413 The age data on the formation of thick peat and humus layer on the QTP, as listed in the **Supplementary**  
414 **materials**, are largely grouped in the LHMP, indicating a warm and wet climate. Along the QTH, the <sup>14</sup>C-

415 age of the humus soil at the depth of 4.4 m in the Borehole No. 8 at Xidatan is  $7,530\pm 300$  a BP, and that of  
416 ash-like humic sand on the first terrace of Nachitai is  $4,910\pm 100$  a BP; anthropic fire-used ash sites have  
417 been found in many places from Nachitai to Xidatan along the Kunlun River, indicating a suitable climate  
418 and environment for human activities; the age of humus layer at the HMSS 109 on the southern slopes of  
419 Tanggula Mountains is  $5,058\pm 443$  a BP, and that at HMSS 120 is  $4,313\sim 4,576$  a BP; the completion time  
420 for the continuous deposition of thick peat was  $3,050\pm 120$  a BP at Qinongga, Yangbajiang, Tibet  
421 Autonomous Region and  $3,575\pm 80$  a BP at Wuma Qú (River), Damxun, Tibet Autonomous Region.

422 On the northeastern and eastern QTP, the middle part of a 2-m-thick humus soil profile on the eastern  
423 slope of Mount Ri'yueshan is dated at  $4,920\pm 80$  a BP while the peat at the depth of 2 m in a 5-m-thick peat  
424 soil profile on southern slope of Heka South Mountains is dated at  $4,625\pm 117$  a BP. A thick humus soil is  
425 dated at  $4,395\pm 215$  a BP at a gelifluction tongue in the Wenbo South Mountains in Shiqu, Sichuan Province,  
426 while the peat is dated at  $5,422\pm 94$  a BP in the lower part of a 4.15-m-thick peat deposit on the morainic  
427 platform in the Nianbao'yeze Mountains. A layer of 5.2 m of peat was deposited during  $9,350\sim 370$  a BP in  
428 the Peat Farm soil profile in the outskirts of Hongyuan, Zoigé Plateau, Sichuan Province, and a layer of 3.3  
429 m peat was formed during  $6,350\sim 3,250$  a BP (Sun, 1998).

430 The above-mentioned extensive and thick deposits are all products in the LHMP as long as  $4,000\sim 5,000$   
431 years. They appear to be an indirect indicator of large-scale and intensive degradation of permafrost. In the  
432 later LHMP (ca.  $4,000\sim 3,000$  a BP), the LLP was  $300\sim 500$  m higher than today; to the north of Kunlun  
433 Mountains and to the south of Tanggula Mountains, permafrost had been converted into seasonally frozen  
434 ground. In the Chumar'he High Plain between the Kunlun and Tanggula mountains, permafrost was thawing  
435 continuously for a long time, reaching to a depth of  $14\sim 16$  m (Jin *et al.*, 2007a) and resulting in a vertical  
436 detachment of permafrost from the active layer (Jin *et al.*, 2006). In the meantime, a thick-layered ground  
437 ice was formed at depths of  $14\sim 16$  m, *i.e.*, the position of paleo-permafrost table (Xin and Ou, 1983). Due  
438 to the thawing of shallow permafrost and ground ice, numerous thermokarst lakes and depressions were  
439 formed, and ice wedge pseudomorphs were formed after ice melting, on the QTP.

440 During the LHMP, permafrost on the plateau was sporadic and isolated, or deeply buried (Jin *et al.*,  
441 2009). However, at high elevations, such as in the Kunlun, Fenghuoshan and Tanggula mountains, it was  
442 still dominated by continuous permafrost. In the meantime, permafrost degraded more intensely on eastern  
443 QTP as represented by that along the Qinghai-Kang (W Sichuan) Highway (QKH) than that in the interior  
444 QTP as represented by that along the QTH and western QTP. Along the QKH, permafrost was completely  
445 converted to seasonally frozen ground at elevations lower than 4,200 m asl; that at  $4,200\sim 4,400$  m asl  
446 (Hua'shixia to Qingshui'he), permafrost thawed down to depths of  $15\sim 25$  m, with a 3-dimensional thawing  
447 (vertical and lateral) (Jin *et al.*, 2006, 2009; Chang *et al.*, 2017). In the end, deeply buried permafrost was  
448 left at depths of  $10\sim 20$  m in some well-preserved areas in the Bayan Har and Anemaqên mountains along  
449 the QKH, and in the Source Area of the Yellow River (Jin *et al.*, 2006a, 2009). In some areas further to the  
450 east, permafrost was thawed completely at lower elevations, leaving behind only some isolated permafrost  
451 islands on the top of Bayan Har and Anemaqên mountains.

452 In mountainous areas in western China, such as in the Tianshan, Altain and Qilian mountains, if  
453 calculated by an elevation of the LLP by  $300\sim 500$  m, permafrost could only be preserved on the top or upper  
454 parts of these high mountains. The Tarim, Turpan and Zhunger basins are at  $41^\circ\sim 46^\circ\text{N}$ , similar to that of  
455 Songhuajiang-Liao'he Basin in Northeast China. Thus, permafrost should have vanished in the major basins  
456 during the LHMP. Calculations based on Figure 2 indicate only an areal extent of  $800,000\sim 850,000$  km<sup>2</sup> for  
457 the remained permafrost in China during the late LHMP, or about 50% of existing permafrost extent at  
458 present.

459 During the late LHMP, westward shifts of vegetation zones occurred under a warming and wetting  
460 climate; it was accompanied also by vertical and horizontal shifts as well. In the peripheries of high mountains  
461 and plateaux, timberline lowered, while in West China, steppes expanded and deserts shrank. The transition  
462 zone (meadowy steppes) between forest and steppe belts evidently moved westwards to northeast of  
463 Manzhouli-Buhat Banner-Hoh Hot-Helanshan South-Xi'ning, a westward movement of  $3\sim 5^\circ\text{E}$  in



464 comparison with today. In the meantime, the boundary between temperate forest-steppe and typical steppe  
465 also shifted westward by 3~4°E. Forest-steppe environment dominated the Altai and Tianshan mountains,  
466 while plateau steppe and forest dominated the QTP. The areal extent of semi-deserts and deserts dramatically  
467 shrank, with only some patches remaining in the middle Tarim Basin, middle and western Inner Mongolia  
468 Plateau and Chaidam Basin. Vegetation zones on southern and eastern QTP, such as in the Hengduan  
469 Mountains, also shifted to varied extents (Tang and Shen, 1996).

#### 470 **4.4 Neoglaciation in the late Holocene (4,000~3,000 to 1,000 a BP) : second major permafrost expansion**

471 In the late Holocene (4,000~3,000 a BP), climate started cooling again. The ice-core record from the  
472 Dunde Glacier in the Qilian Mountains indicates a cooling started ca. 4 ka BP, and reached the coldest period  
473 during 2,800~2,700 a BP. Hence, the cooling fluctuated until 1,000 a BP. This is the so-called Neoglaciation  
474 period in the late Holocene. With the uplifting QTP, climate kept cooling, and mountain glaciers advanced  
475 extensively. Three to four terminal and lateral moraines were left behind in the Kunlun and Tanggula  
476 mountains, such as the Neoglacial lateral moains dated at 3,983~3,522 a BP in the Congce Ice Cap in the  
477 Kunlun Mountains (Zheng, 1990).

478 A string of pinos were formed at 4,250~4,300 m asl along the fault in eastern Xidatan along the QTH;  
479 intensive cryoturbations were developed at about 3,800 m asl on the first terrace of the Kunlun River south  
480 of Nachitai along the QTH. The thick layer of humus formed during the LHMP near the HMSSs 100 and  
481 120 on southern slopes of Tanggula Mountains were re-frozen. Pingo groups 40 km east of Shiqu County  
482 Town, Sichuan Province on eastern QTP were formed at 2,925±175 a BP; those at the northern side of  
483 K65 along the Maqên-Changma'he Highway were formed at 3,925±185 a BP. Large polygons,  
484 gelifluctions and stone circles, and othe periglacial phenomena were extensively developed during the  
485 Neoglaciation period, such those on the Mt. Ri'yueshan (>3,450 m asl), Öla Mountain Pass (>3,750 m asl)  
486 along the QKH and northern slopes of the Bayan Har Mountains (4,000~4,100 m asl). All these paleo-  
487 permafrost and periglacial remains prove a relatively cold climate, when a 20-m-thick permafrost was  
488 developed near the Borehole No. 8 in Xidatan along the QTH.

489 By comparing spatiotemporal variations in these periglacial remains, it can be deduced that the LLP  
490 was then 300 m lower than that of present, and the MAAT, about 2°C lower than today. On the basis of  
491 intensive degradation of permafrost during the LHMP, permafrost reappeared, and expanded radially from  
492 the interior QTP, and reached the maximum permafrost extent in the Neoglacial period by 1,000 a BP, which  
493 was about 20%~30% larger than today. In the Neoglacial period, along the QTH the northern LLP was at  
494 3,700~3,800 m asl south of Nachitai, and the southern LLP was at 4,400~4,500 m asl in the Damxung Valley.  
495 On the Chmar'he High Plain between the Kunlun and Tanggula mountains (>4,500 m asl), permafrost  
496 refroze downwards, forming a layer of epigenetic permafrost 30 m in thickness (Ding and Guo, 1982). This  
497 layer was detached with the residual permafrost of the LHMP. Therefore, so far there has been no buried or  
498 double-decked permafrost found on the Chumar'he High Plain along the QTH.

499 This contrasts with many places on northeastern QTP, such as Hua'shixia to Qingshui'he along the QKH,  
500 and to the east where buried permafrost and thawed nuclei (talik) have been discovered. This might be  
501 attributed to the fact that these areas are on the eastern margins of the plateau permafrost zone, and downward  
502 thawing during the LHMP reached depths of 15~25 m, but the epigenetic permafrost of Neoglaciation was  
503 thinner than 15~25 m, resulting in vertical detachment of permafrost and resultant buried and/or double-  
504 decked permafrost layers. It is also possible that in some areas, due to secondary (second-tier) climate  
505 warming, the Neoglacial permafrost was thawed to certain depths, resulting a mosaicked distributive features  
506 of interwoven multilayered permafrost and taliks (Jin *et al.*, 2006a, 2007a, 2009; Chang *et al.*, 2017). Cold  
507 air drainage could possibly be involved.

508 On the first terrace south of Yituli'he (50°32'N, 129°29'E) in the northern Da Xing'anling Mountains,  
509 Neoglacial ice wedges have been discovered and <sup>14</sup>C-dated at 3,600-1,600 a BP, indicating three cooling  
510 periods of 2,800 a BP (2.1 °C), 2,300 a BP (1.1 °C) and 1,900 a BP (1.3 °C) (Yang and Jin, 2010; Yang *et al.*,



511 2015). It thus concluded that there was a cooling of about 2°C, and a southward shift of the SLP by about  
512 2°N.

#### 513 **4.5 Medieval Warming Period (MWP) (1,000 to 500 a BP): relative Permafrost degradation**

514 After the Neoglaciation, China experienced several small-scale climate fluctuations, among which the  
515 Sui and Tang dynasties (AD 581-907) were in warm periods. The warming started in Shang Dynasty (ca.  
516 1,600 BC to 1,046 BC), reached maxima in Zhou (ca. 1,46 BC to 221 BC), Han (202 BC to AD 220) and  
517 till Tang dynasty (AD 618-907), with a warming of about 1.5°C for centuries, but there were also cooling in  
518 the Sui Dynasty (AD 581-618), and cooling kept to South and North States (AD 420-589) when it was cooler  
519 than today (Zhu, 1972). Because of short history to date, most paleo-periglacial landforms of this period  
520 were well preserved and the remains of paleo-permafrost were distinct on the QTP.

521 Pingos formed in Xidatan, K40 East of Shiqu, West Sichuan Province and K65 along the Maqên-  
522 Changma'he Highway during the Neoglaciation were thawed, forming pingo scars. The humus soils in the  
523 center of thawed depressions were dated at about 720~625 a BP, when permafrost had been thawed at these  
524 locations.

525 This was a period for regional permafrost degradation on the QTP. Downward thawing of permafrost  
526 reached the depth of about 10 m at lower elevations. For example, the lower layer of permafrost, as revealed  
527 at depths of 9.7~12.3 m in Borehole CK1 in Dinaran northeast of Huashixia and at depths of 11.6~15.2 m  
528 in Borehole ZK8 in Changma'he, was the residual permafrost during the MWP (Jin *et al.*, 2006a, 2007a).

529 Accordingly, the upper layer of permafrost as found at depths of 7.5~9.0 m on the Chumar'he High  
530 Plain, and in the Fenghuoshan Mountains in particular along the QTH, was formed during the MWP. For  
531 example, there were two positions of paleo-permafrost tables in the Borehole CK224 on the Chumar'he  
532 High Plain: the upper one of the MWP at 8.4 m in depth, and the lower one of the LHMP at 16 m. Thick-  
533 layered ground ice were all identified under these permafrost tables (Xin and Ou, 1983). The degradation of  
534 permafrost during the MWP resulted in a higher LLP of about 150~250 m above the present LLP, while the  
535 SLP moved northwards by 1~2°N. As a result, the permafrost extent in China during the MWP was about  
536 20% less than today.

#### 537 **4.6 Little Ice Age (LIA, 500 to 100 a BP) in the late Holocene: Relative permafrost expansion**

538 The Little Ice Age (LIA) is the cold period in the 15<sup>th</sup> ~ 19<sup>th</sup> century, with the latest permafrost  
539 expansions and glacier advances, which was recorded in ice-cores and glacial deposits. In the ice-cores from  
540 the Dunde Glacier No. 1 in the Qilian Mountains, the three coolings occurred in AD 1420~1520, 1570~1680,  
541 and 1770~1890. The second cold period (16<sup>th</sup> and 17<sup>th</sup> centuries) was the coldest among the three, with a  
542 cooling of about 1.5°C colder than today.

543 It was a time when the QTP was drying and cooling, which was accompanied by permafrost expansion  
544 and thickening, and new permafrost islands were formed in the peripheries of the QTP. Along the QTH, a  
545 permafrost layer was formed by the downward freezing, which was re-attached with the upper paleo-  
546 permafrost (table) formed during the MWP in the late Holocene. For example, the humus layer at the HMSS  
547 121 along the QTH formed since the last 780 a BP was refrozen. On eastern QTP, the thin permafrost of the  
548 LIA was unable to attach to the underlying permafrost layer, such as the permafrost layer found at depths of  
549 1.5~8.0 m in Borehole ZK6 on the northern bank of the Ngöring Lake and at depths of 5.3~8.2 m in the  
550 water well in the Qingshui'he Town on the southern slope of the Bayan Har Mountains along the QKH (Jin  
551 *et al.*, 2006a, 2006b)

552 Active rock glaciers, block fields, stone stripes, or other similar sorted patterned ground or ice-  
553 contained permafrost can indicate the occurrence of permafrost (Tian, 1981; Gao, 1983). Barsch (1978) first  
554 pointed out that rock glaciers could indicate the LLP of discontinuous alpine permafrost. Therefore, Jakob  
555 (1992) estimated the LLP of discontinuous alpine permafrost at about 5,560-5,360 m asl (sunny slopes) and  
556 4,959-5,050 m asl (shadowy slopes) in the Kunbu Himalayas, Nepal on the basis of active rock glaciers and

557 seismic geophysical data in the vicinity of Poklade Cliff (27°55'N, 86°50'E), whereas the lower limit of  
558 active rock glaciers there is at about 5,000~5,300 m asl. These results agree well with the calculated result  
559 from the Gauss curve for the location ( $\geq 5,080$  m asl, 25°22'N) (Cheng and Wang, 1982). On the basis of  
560 the distribution of proglacial and morainic rock glaciers, Owen and England (1998) deduced that the LLP of  
561 discontinuous permafrost should be higher than 4,000 m asl in western Himalayas and Karakurums in  
562 northern Pakistan and India. Similarly, it can be deduced that during the LIA, (inactive) stone fields and  
563 (inactive) stone stripes were above 4,130 m asl along the road side of Rizha Village, Darag County, Qinghai  
564 Province. At the lower limit of these stone fields and stripes, the underlying humic soils are dated at  $422 \pm 85$   
565 a BP, which should be older than the overlying stone streams or stripes. Therefore, those inactive stone fields  
566 and stone stripes/streams were formed during the LIA. At present, the LLP at this location is at 4,300 m asl.  
567 Thus, the LIA had a cooling of about 1.0~1.5°C, a lowering of LLP by 150~200 m, and with a permafrost  
568 extent of  $1.5 \times 10^6$  km<sup>2</sup>, or about 15%~20% greater than today.

569 During the LIA, plateau lakes shrank continuously, and some small and medium lakes dried up. Most  
570 of the lakes became saline and salt lakes, such as the salt lake behind the HMSS 69 along the QTH, where  
571 silty soil under a 60-cm-thick salt crust was dated at  $1,094 \pm 433$  a BP; the silt under a 50-cm-thick salt layer  
572 in the Hajiang Salt Lake to the east of Ngöring Lake was dated at  $1,080 \pm 260$  a BP. In the meantime, those  
573 (semi)fixed sand dunes were re-activated on the surface, and covered by aeolian sand, result in worsening  
574 land desertification.

#### 575 **4.7 Recent warming (since 100 a BP, i.e., the 20<sup>th</sup> century): persistent permafrost degradation**

576 During the last century, especially the last few decades, the effect of greenhouse gases may have caused  
577 and sustained climate warming. Large amounts of data indicate a global warming of about 0.3~0.8°C since  
578 AD1880; in particular, the climate since the 1980s has been the warmest since the meteorological record  
579 was commenced. During the last four decades, the MAAT in the permafrost regions on the QTP has risen  
580 by 1.12°C, at a warming rate of 0.025~0.030°C/a, much greater than that of the periphery non-permafrost  
581 regions (0.017~0.019°C/a) (Jin *et al.*, 2011a). Particularly, since the 21<sup>st</sup> century, the climate warming has  
582 been accelerated, and mean annual ground surface temperature has risen by 1.34°C. The climate in  
583 Northeast China has risen by 1.7°C during the last 100 years, in which the Da Xing'anling Mountains has  
584 experienced the most pronounced warming: the last three decades in the 20<sup>th</sup> century have witnessed a rise  
585 in MAAT by 1.4~2.0°C. It is evident that during the last six decades, there have a clear pattern in changes  
586 in ground surface temperatures. There was a cold period during the 1950s to 1970s, followed by a warming  
587 since the 1980s; the coldest occurred in the 1950s, with a departure of -0.8°C; the warmest occurred in the  
588 2000s, with a departure of +1.1°C. However, the climate warming again was the most pronounced in the  
589 Da Xing'anling Mountains, with a warming rate of 0.038~0.040°C/a in the MAAT during the last 30 years  
590 (Luo *et al.*, 2014). Climate warming has resulted in persistent permafrost degradation, and particularly  
591 since the 21<sup>st</sup> century, permafrost degradation has been accelerating. Areal extent of permafrost in China  
592 has been reduced to  $1.59 \times 10^6$  km<sup>2</sup> from  $1.59 \times 10^6$  km<sup>2</sup> (Zhou *et al.*, 2000; Ran *et al.*, 2012).

#### 593 **4.8 Changes of permafrost in China during the last 20 ka: patterns, processes and trends**

594 In summary, since the LLGM although there have been occasional permafrost expansions in cold  
595 periods, such as the Neoglaciation and LIA, the areal extent of permafrost in China in general has been on  
596 the decline under a fluctuatively warming climate (Table 1). The areal extent of permafrost during the LLGM  
597 was close to its maximum at 20 ka BP and the LHMP could have reached its minimum, despite the  
598 substantial expansions during the Neoglaciation and LIA. During the MWP and since the last century, China  
599 has witnessed the most intensive, rapid and extensive permafrost degradation since the LHMP, and this trend  
600 is currently being enhanced. Because of these changes, the areal extent of permafrost in China has shrunk  
601 from  $5.30 \times 10^6$ ~ $5.40 \times 10^6$  km<sup>2</sup> at the LLGM/LLPMax to  $0.80 \times 10^6$ ~ $0.85 \times 10^6$  km<sup>2</sup> at the LHMP/LLPMin, and  
602 then back to the present  $1.59 \times 10^6$  km<sup>2</sup>.

Table 1. Summary of changes in permafrost in China during the last 20 ka

Climate period	Absolute age	Changes in pf features	Climate & cooling (°C)	Change in SLP (°N)	Change in LLP (m)	Pf extent (10 <sup>6</sup> km <sup>2</sup> )	Percent of today (%)	Major direct evidence	Major indirect evidence	Major references
Local Last Glacial Max (LLGM) in Late Pleistocene	~20 to 13~10.8 ka BP	Ice-wedges developed over the entire permafrost area	Cold/dry, 4-5 (NE China), 3-11 (N China), 7-9 (QTP)	S ↓4-5 (NE China)	↓1200-1400	5.3-5.4	>300	Cryogenic wedges of all types	Glacial landforms, ice cores, paleo-timberline, pollen, sandland, cold climate fauna & flora, models	Zhang, 1983; Xu & Pan, 1990; Wang & Bian, 1993; Tong, 1993; Pan & Chen, 1997; Cui <i>et al.</i> , 2004; Cheng <i>et al.</i> , 2006; Jin <i>et al.</i> , 2006a, 2007a, 2016; Chang <i>et al.</i> , 2011, 2017; Zhao <i>et al.</i> , 2013
Dramatic climate changes in early Holocene	10.8 to 8.5~7 ka BP	Relative stable & degrading permafrost	Drying/cooling, then warming/wetting, very unstable	Retreat, started to disappear on Sanjiang Plain	↑600-700	2.2-2.4	140-150	Pingo scars, sand wedges	Ice core, diatom, pollen, peat, sand dunes, ...	Li, 1982; Wang, 1989; Li & Jiao, 1990; Song & Xia, 1990; Yao & Shi, 1992; Tang & Shen, 1996
MidHolocene Megathrmal Period (LHMP)	8.5~7 至 4~3 ka BP	Intensive degradation	Wet/warm, 2~3 (most parts), 4~5 (QTP), 1.0~3.5 (N China)	↑N 3-4 (NE China)	↑300-500 (QTP, mts. in W China)	0.8-0.85	50	Ice wedges, buried pf, ground ice, thermokarst lakes, paleopf, gelifluctions, pingo scars	Mineral analysis, peat, ice-core (δ <sup>18</sup> O), sand dunes, human fire use, timberline, pollens	Guo <i>et al.</i> , 1981; Xing & Ou, 1983; Tong, 1993; Tang & Shen, 1996; Sun, 1998; Jin <i>et al.</i> , 2006a, 2007a; 2009, 2016; Shi <i>et al.</i> , 2006; Yu <i>et al.</i> , 2013
Late Holocene cold period (Neoglaciation)	4~3 to 1 ka BP	2 <sup>nd</sup> expansion	Fluctuatingly cooling -2 ~ -1 (NE China, QTP)	S ↓2 (NE China)	↓~300 (青藏)	1.9-2.1	120-130	Pingo scars, cryoturbations, polygons, gelifluctions, ice wedges	Ice core, glacial till, peat, detached or buried pf	Ding & Guo, 1982; Zheng, 1990; Jin <i>et al.</i> , 2007a, 2009, 2011b, 2016; Yang & Jin, 2010; Yang <i>et al.</i> , 2015; Chang <i>et al.</i> , 2017
Late Holocene warm period (MWP)	1~0.5 ka BP	Relative retreat	Wet/warm, 1.5	↑N 1~2	↑~150-250	1.4-1.5	80	Pingo scars, buried pf, ground ice	Phenology, humus	Zhu, 1972; Xing & Ou, 1983; Jin <i>et al.</i> , 2006a, 2007a
Little Ice Age (LIA)	500~100 a BP	Relative expansion	Fluctuatingly cooling -1.5~ -1	S ↓1~1.5	↓~150-200	2.1-2.2	115-120	Paleopf, detached pf, stone fields & streams	Ice-core, till, humus, silt in salt lake, sand land	Jin <i>et al.</i> , 2006a
Recent warming	100~0 a BP	Persistent degradation	Warm/dry 0.3~0.8	↑N 0.5-1.5	↑50~100	1.59	100	Ground temp, LLP/SLP, areal extent survey and measurement	Measurement and thermokarsts	Jin <i>et al.</i> , 2006a, 2011b, 2016; Ran <i>et al.</i> , 2012

605 **5. Conclusions and prospects**

606 Since the last 20 ka, China has experienced many major climatic, environmental and geocryological  
607 changes, such as the LLGM/LLPMax at the end of the Late Pleistocene and the LHMP/LLPMin in mid-  
608 Holocene. On the basis of paleo-permafrost and periglacial remains, in combination with glacial,  
609 palentological and other records, it is estimated that during the LLGM, in comparison with today, the MAAT  
610 was about 7~9°C colder on the QTP, 4~5°C colder in the Da and Xiao Xing'anling Mountains, and 5~12°C  
611 colder in arid regions in North China; during the LHMP/LLPMin, in comparison with today, the MAAT  
612 was about 4~5°C warmer on the QTP, 3~4°C warmer in the Xing'anling Mountains, and 1~3.5°C colder in  
613 arid regions in North China. Accordingly, permafrost has changes substantially. The latest data indicate a  
614 present extent of permafrost in China at  $1.59 \times 10^6$  km<sup>2</sup>, shrinking from  $5.3 \times 10^6 \sim 5.4 \times 10^6$  km<sup>2</sup> during the  
615 LLGM/LLPMax, or three times of today. However, during the LHMP/LLPMin, that was reduced to  
616  $0.80 \times 10^6 \sim 0.85 \times 10^6$ , or about 50% of the current permafrost area. That in other periods falls in between the  
617 LLPMax and LLPMin.

618 According to the ages and distributive features of paleopermafrost in China, after the delineation of  
619 permafrost patterns in the LLPMax/LLPMin, the evolutionary processes of permafrost in China can be  
620 divided into seven periods: (1) LLGM/LLPMax in the Late Pleistocene (~20 to 13~10.8 ka BP); (2) Dramatic  
621 changes in climate and permafrost in early Holocene (10.8 to 8.5~7 ka BP); (3) local Mid-Holocene  
622 Megathermal Period (LHMP, 8.5~7 to 4~3 ka BP); (4) Late Holocene cold period, or Neoglaciation (4~3 to  
623 1 ka BP); (5) Late Holocene warm period (Medieval Warm Period, MWP, 1,000 ~ 500 aBP); (6) Late  
624 Holocene cold period (Little Ice Age, LIA, 500~100 a BP), and; (7) Recent warming period (118~0 a BP,  
625 20<sup>th</sup> century upto date). Paleo-climate, -geography and -environment, and permafrost features were  
626 reconstructed for the seven periods.

627 The formation, development and changes of permafrost in China are complicated due to the combined  
628 influences from climate changes of varied spatiotemporal scales and human activities and subsequent  
629 interwoven impacts. They have resulted in concurrent processes of permafrost formation and development  
630 as well as degradation at the same time in different regions and at different depths. This is particularly true  
631 for shallow permafrost and the permafrost layer in the peripheries of permafrost zones where climatic  
632 fluctuations of different amplitudes and intensity have induced repeated freezing and thawing, forming  
633 mosaicked distributive patterns of permafrost and talik. As a result, the dating of permafrost remains a major  
634 challenge in Quaternary geocryology in China. In particular, rapid, large-scale and intensive economic  
635 development have tremendous adverse impacts on Quaternary permafrost and periglacial landforms, it  
636 deems necessary to timely rescue and study these precious evidence and records.

637 Permafrost should have developed in Tarim and Zhunger basins in Xinjiang, West China during the  
638 LLGM/LLPMax taking into account of their latitudes and elevations. However, so far no reliable paleo-  
639 permafrost and -periglacial evidence has been discovered in the interiors of the two basins. Was there  
640 permafrost in history? This is also true for other sand lands and deserts/gobi in North China and adjacent  
641 regions or countries. The relationships between permafrost and deserts in China and bordering regions await  
642 for reliable data and further investigations.

643 **Acknowledgments**

644 Supported by the joint program of National Natural Science Foundation of China (NSFC) and Russian Foundation for  
645 Basic Research (FRBR) on “*Formation, evolution and changes of Pleistocene cryogenic deposits in Eastern Asia*”  
646 (Grant No. 41811530093), Subproject No. XDA05120302 (*Permafrost extent in China during the Last Glaciation Max-*  
647 *imum and Megathermal*) of the Strategic Pilot Science and Technology Program of the Chinese Academy of Sciences  
648 (CAS), and the *CAS Overseas Professorship of Sergey S. Marchenko*, and under the auspices of the International Per-  
649 *mafrost Association Working Group on Global Permafrost Extent During the Last Permafrost Maximum (LPM)*. In  
650 addition, authors greatly appreciate the support of Professor Hua'yu Lu at the Nanjing University in timely providing  
651 the OSL dating; remarks and advice from Academician Zhengtang Guo and other colleagues in the Strategic Pilot Sci-  
652 *ence and Technology Program of the Chinese Academy of Sciences* (Grant No. XDA05000000, *Identification of carbon*  
653 *budgets for adaptation to changing climate and the associated issues*). Authors also would like to thank two unidentified  
654 reviewers for their constructive review opinions.

- 656 Barsch D, 1978. Rock glaciers as indicators of discontinuous alpine permafrost. An example from the Swiss Alps.  
657 [Proceedings, 3<sup>rd</sup> International Conference on Permafrost](#), National Academy Press, Washington DC, pp. 136-141.
- 658 Böhner J, Lehmkuhl F, 2005. Environmental change modelling for central and high Asia: Pleiocene, present and future  
659 scenarios. [Boreas](#), 34: 220-231
- 660 Chang X, Jin H, He R, 2011. Formation and environmental evolution of sand wedges on the Tianshuihai North  
661 lakeshore in the western Kunlun Mountains. [Quat Sci](#), 31(1): 112-119 (in Chinese)
- 662 Chang X, Jin H, Zhang Y, He R, Luo D, Wang Y, Lü L, 2015. Thermal impacts of boreal forest vegetation on active  
663 layer and permafrost soils in northern Da Xing'anling (Hinggan) Mountains, Northeast China. [Arct, Antarct Alp  
664 Res](#), 47(2): 267-279
- 665 Chang X, Jin H, Wang S, 2017. Evolution of permafrost on the Qinghai-Tibet Plateau and its impacts on aeolian  
666 environments. [Sci Cold Arid Reg](#), 9(1): 1-19
- 667 Cheng G, Wang S, 1982. On the zonation of high-altitude permafrost in China. [J Glaciol Cryopedol \(Geocryol\)](#), 4(2):  
668 1-17 (in Chinese)
- 669 Cheng J, Zhang X, Tian M, Yu W, Tang D, Yue J, 2006. Ice wedge casts discovered in the source area of Yellow  
670 River, northeast Tibetan Plateau and their paleoclimatic implications. [Quat Sci](#), 26(1): 92-98 (in Chinese)
- 671 Cui Z, 1980. Periglacial phenomena on the Qinghai-Tibet Plateau and their environmental significance. In: [Collection  
672 Papers for International Communications on Geology \(5\)](#). Beijing: Geology Press, pp. 109-122 (in Chinese)
- 673 Cui Z, Zhao L, Vandenberghe J, Zhang W, 2002. Discovery of ice wedge and sand-wedge networks in Inner Mongolia  
674 and Shanxi Province and their environmental significance. [J Glaciol Geocryol](#), 24(6): 708-717 (in Chinese)
- 675 Cui Z, Yang J, Zhao L, Zhang W, Xie Y, 2004. Discovery of a large area of ice-wedge networks in Ordos: Implica-  
676 tions for the southern boundary of permafrost in the north of China as well as for the environment in the latest 20  
677 kaBP. [Chin Sci Bull](#), 49(11): 1177-1184. DOI: 10.1360/03wd0211
- 678 Ding D, Guo D, 1982. Preliminary discussions on the evolutionary history of permafrost on the Qinghai-Tibet Plateau.  
679 In: [Geographical Society of China ed., Proceedings of Chinese Conference on Glaciology and Geocryology \(Ge-  
680 ocryology Volume\)](#). Beijing: Science Press, pp. 78-82 (in Chinese)
- 681 Du N, Kong Z, Shan F, 1989. A preliminary investigation on the vegetational and climatic changes since 11,000 years in  
682 Qinghai Lake-An analysis based on palynology in core QH85-<sup>14</sup>C. [Act Botan Sin \(J Integrat Plant Biol\)](#), 30(10):  
683 803-814+825-826 (in Chinese)
- 684 French H M, 2018. [The Periglacial Environment \(4<sup>th</sup> Edition\)](#). John Wiley & Sons, p. 1-515
- 685 Gao F, 1983. Ancient rock sea in Shennongjia Mountain. [J Glaciol Cryopedol \(Geocryol\)](#), 5(4): 67-69 (in Chinese)
- 686 Guo D, Li Z, 1981. Preliminary approach to the history and age of permafrost in Northeast China. [J Glaciol Cryopedol  
687 \(Geocryol\)](#), 3(4): 1-14 (in Chinese)
- 688 Guo D, Wang S, Lu G, Dai J, Li E, 1981. Division of permafrost regions in Daxiao Hinggan Ling, Northeast China. [J  
689 Glaciol Cryopedol \(Geocryol\)](#), 3(3): 1-9 (in Chinese)
- 690 Harris S A, Jin H J, 2012. Tessellons and sand wedges on the Qinghai-Tibet Plateau and their palaeo-environmental  
691 implications. [Proc, 10<sup>th</sup> Int Conf on Permafr](#), Salehard, Russia, 26-29 June 2012, Vol. 1: 149-154
- 692 Harris S A, Jin H J, He R X, 2016. Very large cryoturbation structures of Last Permafrost Maximum age at the foot of  
693 Qilian Mountains (NE Tibet Plateau, China): A discussion. [Permafr Periglac Process](#), 28(4): 757-762
- 694 Harris S A, Brouckov A, Cheng G, 2017. [Geocryology--Characteristics and use of frozen ground and permafrost  
695 landforms](#). CRC Press, p.1-765.
- 696 Harris S A, Jin H, He R, 2018. Tessellons, topography, and glaciations on the Qinghai-Tibet Plateau. [Sci Cold Arid Reg,  
697 10\(3\): in press.](#)
- 698 Heyman J, 2010. Paleoglaciology of the northeastern Tibetan Plateau. [Doctoral Dissertation at the Department of  
699 Physical Geography and Quaternary Geology, Stockholm University](#), 1-11
- 700 Heyman J, Hättestrand C, Stroeven A P, 2008. Glacial geomorphology of the Bayan Har sector of the NE Tibetan Plateau.  
701 [J Maps](#), 4(1): 42-62
- 702 Heyman J, Stroeven A P, Alexanderson H, Hättestrand C, Habor J, Li Y K, Caffee M W, Zhou L P, Veres D, Liu F,  
703 Machiedo M, 2009. Paleoglaciation of Bayan Har Shan, northeastern Tibetan Plateau: glacial geology indicates  
704 maximum extents limited to ice cap and ice field scales. [J Quat Sci](#), 24: 710-727



- 705 Jakob M, 1992. Active rock glaciers and the lower limit of discontinuous alpine permafrost, Khumbu Himalaya, Nepal.  
706 [Permafr Periglac Process](#), 3: 253-256
- 707 Jiao S, Wang L, Sun C, Yi C, Cui Z, Liu G, 2015. Discussion about the variation of permafrost boundary in Last Glacial  
708 Maximum and Holocene Megathermal, Tibetan Plateau. [Quat Sci](#), 35(1): 1-11 (in Chinese)
- 709 Jiao S, Wang L, Liu G, 2016. Prediction of Tibetan Plateau Permafrost Distribution in Global Warming. [Act Sci Natur](#)  
710 [Universit Pekinen](#), 52(2): 249-256 (in Chinese)
- 711 Jin H, Zhao L, Wang S, Guo D, 2006a. Evolution of permafrost and environmental changes of cold regions in eastern  
712 and interior Qinghai-Tibetan Plateau since the Holocene. [Quat Sci](#), 26(2): 198-210 (in Chinese)
- 713 Jin H, Zhao L, Wang S, Jin R, 2006b. Thermal regimes and degradation modes of permafrost along the Qinghai-Tibet  
714 Highway. [Sci Chin](#), 49(D11): 1170-1183
- 715 Jin J, Chang X, Wang S, 2007a. Evolution of permafrost on the Qinghai-Tibet Plateau since the end of the Pleistocene.  
716 [J Geophys Res](#), 112: F02S09. DOI: 10.1029/2006JF000521
- 717 Jin H, Yu Q, Lü L, Guo D, Li Y, 2007b. Degradation of permafrost in the Xing'anling Mountains, Northeastern China.  
718 [Permafr Periglac Process](#), 18(2): 245-258
- 719 Jin H, He R, Cheng G, Wu Q, Wang S, Lü L, Chang X, 2009. Change in frozen ground and eco-environmental impacts  
720 in the Sources Area of the Yellow River (SAYR) on the northeastern Qinghai-Tibet Plateau, China. [Env Res Lett](#),  
721 4: 045206. DOI: 10.1088/1748-9326/4/045206
- 722 Jin H, Luo D, Wang S, Lü L, Wu J, 2011a. Spatiotemporal variability of permafrost degradation on the Qinghai-Tibet  
723 Plateau. [Sci Cold Arid Reg](#), 3(4): 281-305
- 724 Jin H, Chang X, Guo D, Yang S, He R, 2011b. Holocene sand soil wedges on the south-central Hunlun Buir High Plain  
725 in Northeast China. [Quat Sci](#), 31(5): 765-779 (in Chinese)
- 726 Jin H, Chang X, He R, and Guo D, 2016. Evolution of permafrost and periglacial environments in Northeast China since  
727 the Last Glaciation Maximum. [Sci Cold Arid Reg](#), 8(4): 269-296
- 728 Ju L, Wang H, Jiang D, 2007. Simulation of the last glacial maximum climate over East Asia with a regional climate  
729 model nested in a general circulation model. [Paleogeogr, Paleoclimatol, Paleoecol](#), 248: 376-390
- 730 Li B, Li J, Cui Z, Zheng B, Zhang Q, Wang F, Zhou S, Shi Z, Jiao K, Kang J, 1991. [Quaternary glacial distribution map](#)  
731 [of Qinghai-Xizang \(Tibet\) Plateau](#). Science Press, Beijing
- 732 Li F, 1990. Features of paleo-periglacial structures on the Sanjiang Plain, Northeast China and their environmental  
733 implications. In: [Formation and Evolution of Quaternary Natural Environment on NE China Plain, China](#). Harbin:  
734 Harbin Cartography Press, pp. 202-208 (in Chinese)
- 735 Li S, Jiao K, 1990. Glacier variations on the south slope of West Kunlun Mountains since 30,000 years. [J Glaciol](#)  
736 [Geocryol](#), 12(4): 311-318 (in Chinese)
- 737 Li S, He Y, 1990. Basic features of permafrost in the West Kunlun Mountains. In: Lanzhou Institute of Glaciology and  
738 Geocryology, Chinese Academy of Sciences ed., [Collection Papers 4th Chin Conf on Glaciol Geocryology](#)  
739 [\(Geocryology Volume\)](#). Beijing: Science Press, pp. 1-8
- 740 Li X, 1982. <sup>14</sup>C dating of humus layer in the Damxung and Yangbajing basins, Xizang (Tibet) Autonomous Region,  
741 China and its significance. Editorial Committee of the Collection Papers for the Geology of Qinghai-Xizang (Tibet)  
742 Plateau, Ministry of Geology and Minerals, PRC, ed. [Collection Papers for Geology of Qinghai-Xizang \(Tibet\)](#)  
743 [Plateau \(4\): Quaternary Glacial Geology](#). Beijing: Geology Press, pp. 131-136 (in Chinese)
- 744 Liang F, Cheng G, 1984. Polygon-veins along the Qinghai-Xizang Highway. [J Glaciol Geocryol](#), 6(4): 51-60 (in Chinese)
- 745 Liu J, Yu G, Chen X, 2002. Palaeoclimate simulation of 21 ka for the Tibetan Plateau and eastern Asia. [Clim Dynam](#),  
746 19: 575-583
- 747 Luo D, Jin H, Jin R, Yang X, Lü L, 2014. Spatiotemporal variations of climate warming in northern Northeast China as  
748 indicated by freezing and thawing indices. [Quat Int](#), 349: 187-195
- 749 Ma H, 1996. Studies on terraces of the Chaidam basin, and Huangshui and Huanghe (Yellow) rivers. [A PhD Thesis of](#)  
750 [the Lanzhou University](#). Lanzhou, pp. 32-33 (in Chinese)
- 751 Mark B G, Harrison S P, Spessa A, New M, Evans D J A, Helmens K F, 2005. Tropical snowline changes at the last  
752 glacial maximum: a global assessment. [Quat Int](#), 138: 168-201
- 753 Murton J B, Kolstrup E, 2003. Ice-wedge casts as indicators of paleotemperatures: precise proxy or wishful thinking?  
754 [Progr Phys Geogr](#), 27: 155-170

- 755 Owen L A, England J, 1998. Observations on rock glaciers in the Himalayas and Karakoram Mountains of northern  
756 Pakistan and India. *Geomorphology*, 26: 199-213
- 757 Owen L A, Finkel R C, Ma H Z, Spencer J Q, Derbyshire E, Barnard P L, Caffee M W, 2003. Timing and style of  
758 Late Quaternary glaciation in northeastern Tibet. *Geol Soc Am Bull*, 115: 1356-1364
- 759 Owen L A, Finkel R C, Ma H Z, Barnard P L, 2006. Late Quaternary landscape evolution in the Kunlun Mountains and  
760 Qaidam Basin, Northern Tibet: a framework for examining the links between glaciation, lake level changes and  
761 alluvial fan formation. *Quat Int*, 73: 154-155
- 762 Pan B, Chen F, 1997. Permafrost evolution in the northeastern Qinghai-Tibetan Plateau during the last 150,000 years. *J*  
763 *Glaciol Geocryol*, 19(2): 124-132 (in Chinese)
- 764 Qi B, Hu D, Zhao X, Zhang X, Zhang Y, Yang X, Zhao Z, Gao X, 2014. Fossil sand wedges in the northern shore of  
765 Qinghai Lake: discovery and paleoclimatic implications. *J Glaciol Geocryol*, 36(6): 1412-1419 (in Chinese)
- 766 Qiu G, Cheng G, 1995. Permafrost in China: Past and Present. *Quat Sci*, 15(1): 13-22 (in Chinese)
- 767 Qiu S, 1985. Basic features of natural environments in Northeast China Plain during the Pleistocene. *Collection of Papers*  
768 *presented in the Conference on Quaternary Glacial and Periglacial Landforms in China*. Beijing: Science Press,  
769 208-211 (in Chinese)
- 770 Ran Y, Li X, Cheng G, Zhang T, Jin H, 2012. Distribution of permafrost in China: An overview of existing permafrost  
771 maps. *Permafrost Periglacial Process*, 23: 322-333
- 772 Романовский Н Н (Romanovskii N N), 1977. *Формирование полигонально-жильных структур (Formation of*  
773 *Polygonal-Wedge Structures)*. Изд-во Наука, Новосибирск СССР (Science Press, Novosibirsk, USSR), 70-85
- 774 Schmid M O, Baral P, Gruber S, Shahi S, Shrestha T, Stumm D, Wester P, 2015. Assessment of permafrost distribution  
775 maps in the Hindu Kush Himalayas region using rock glaciers mapped in Google Earth. *The Cryosphere*, 9: 2089-  
776 2099
- 777 Shen C, Tang L, Wang S, 1996. Vegetation and climate during the last 250,000 years in Zoigê region. *Act*  
778 *Micropalaeontol Sin*, 13(4): 401-406 (in Chinese)
- 779 Shi Y, 1998. Evolution of the cryosphere in the Tibetan Plateau, China and its relationship with the global change in the  
780 Mid Quaternary. *J Glaciol Geocryol*, 20(3): 197-208 (in Chinese)
- 781 Shi Y (ed.), 2006. *Quaternary glaciers in China and environmental changes*. Beijing: Science Press, pp. 134-138 (in  
782 Chinese)
- 783 Shi Y (Chief ed.), 2011. *New Theories on Quaternary Glaciation*. Shanghai: Shanghai Science Outreach Press, pp. 130-  
784 135 (in Chinese)
- 785 Shi Y, Zheng B, Li S, 1990. Last Glaciation and the Maximum Glaciation in Qinghai-Xizang Plateau. *J Glaciol Geocryol*,  
786 12(1): 1-16 (in Chinese)
- 787 Shi Y, Kong Z, Wang S, Tang L, Wang F, Yao T, Zhao X, Zhang P, Shi S, 1992. Basic features of Climate and  
788 Environment in China during the Holocene Megathermal Period. In Shi Y, Kong Z ed., *Climate and Environment*  
789 *in China during the Holocene Megathermal Period*. Beijing: Science Press, pp. 1-18 (in Chinese)
- 790 Shi Y, Zheng B, Li S, Ye B 1995. Studies on altitude and climatic environment in the middle and east parts of Tibetan  
791 Plateau during Quaternary maximum glaciation. *J Glaciol Geocryol*, 17(2): 99-112 (in Chinese)
- 792 Shi Y, Zheng B, Yao T, 1997. Glaciers and Environments during the Last Glacial Maximum (LGM) on the Tibetan  
793 Plateau. *J Glaciol Geocryol*, 19(2): 97-113 (in Chinese)
- 794 Shi Y, Zheng B, Su Z, 2000. Quaternary glaciations, glaciation periods, and interglacial cycles and environmental  
795 changes. In Shi Y ed., *Glaciers and Environment in China*. Beijing: Science Press, pp. 320-355 (in Chinese)
- 796 Song H, Xia Y, 1990. Pingo Scars and Peatlands on the Sanjiang Plain. *Formation and Evolution of Natural Environment*  
797 *in the NE China Plain, China*. Harbin: Harbin Cartography Press, pp. 209-216 (in Chinese)
- 798 Sun G, Chief ed., 1998. *Marshes and Peat in the Hengduan Mountains*. Beijing: Science Press, pp. 220-224 (in Chinese)
- 799 Sun J, Wang S, Wang Y, Zhou Y, Lin Z, Zhang Q, Chen S, 1985. Paleoenvironment in Northeast China during the Last  
800 Glaciations. *Quat Sci*, 6(1): 82-89 (in Chinese)
- 801 Tang L, Shen C, 1996. Progress in the study of vegetation and climate change since Pliocene in the Qinghai-Xizang  
802 Plateau. *Adv Earth Sci*, 11(2): 198-203 (in Chinese)
- 803 Tang L, Shen C, Kong Z, Wang F, Liu K 1998. Pollen evidence of climate during the Last Glaciation Maximum in  
804 eastern Tibetan Plateau. *J Glaciol Geocryol*, 20(2): 42-44 (in Chinese)

- 805 Tian Z, 1981. A study about the traces of Quaternary glaciations of Mount Taibaishan, Shaanxi Province. *J Northwest*  
806 *Univ*, (3), 67-69 (in Chinese)
- 807 Tong B, 1993. Ice wedges in Northeast China. *J Glaciol Geocryol*, 15(1): 41-46 (in Chinese)
- 808 Vandenberghe J. 1992. Cryoturbations: a sediment structural analysis. *Permafr Periglac Process*, 3: 343-352
- 809 Vandenberghe J, Pissart A, 1993. Permafrost changes in Europe during the Last Glacial. *Permafr Periglac Process*, 4:  
810 121-135
- 811 Vandenberghe J, Cui Z, Zhao L and Zhang W, 2004. Thermal-contraction-crack networks as evidence for late-  
812 Pleistocene permafrost in Inner Mongolia, China. *Permafr Periglac Process*, 15: 21-29
- 813 Vandenberghe J, Wang X, Vandenberghe D, 2016. Very large cryoturbation structures of Last Permafrost Maximum  
814 age at the foot of the Qilian Mountains (NE Tibet Plateau, China). *Permafr Periglac Process*, 27: 138-143
- 815 Wang P, Sun J, 1994. Last glacial maximum in China: Comparison between land and sea. *Catena*, 23: 341-353
- 816 Wang S, 1989. Formation and evolution of permafrost on the Qinghai-Xizang Plateau since the Late Pleistocene. *J*  
817 *Glaciol Geocryol*, 11(1): 67-75 (in Chinese)
- 818 Wang S, Bian C, 1993. The involutions and their palaeoclimatic significance in the Nachitai region along the Qinghai-  
819 Xozang Highway. *Geogr Res*, 132(1): 94-100 (in Chinese)
- 820 Wang X, Vandenberghe D, Yi S, Vandenberghe J, Lu H, Van Balen R, Van den Haute P, 2013. Late Quaternary  
821 paleoclimatic and geomorphological evolution at the interface between the Menyuan basin and the Qilian  
822 Mountains, northeastern Tibetan Plateau. *Quat Res*, 80: 534-544
- 823 Wei G, Hu S, Yu K, Hou Y, Li X, Jin C, Wang Y, Zhao J, Wang W, 2010. New materials of the steppe mammoth,  
824 *Mammuthus trogontherii*, with discussion on the origin and evolutionary patterns of mammoths. *Sci China Earth*  
825 *Sci*, 53: 956-963
- 826 Xin Z, Ou R, 1983. Study on the permafrost table from the changes in contents of salt and clay minerals. Lanzhou  
827 Institute of Glaciology and Geocryology, Chinese Academy of Sciences edited, *Proceedings of the 2<sup>nd</sup> Chinese*  
828 *Conference on Geocryology*. Lanzhou: Gansu People's Press, pp. 158-164 (in Chinese)
- 829 Xu S, Pan B, 1990. Periglacial wedge structures on eastern Qinghai Plateau and their formation environments. In:  
830 Lanzhou Institute of Glaciology and Geocryology, Chinese Academy of Sciences edited, *Proceedings of the 4<sup>th</sup>*  
831 *Chinese Conference on Glaciology and Geocryology (Geocryology Volume)*. Beijing: Science Press, 17-24 (in  
832 Chinese)
- 833 Xu S, Zhang W, Xu D, Xu Q, Shi S, 1984. Discussion on the periglacial development in the northeast margin regional  
834 of Qinghai-Xizang Plateau. *J Glaciol Geocryol*, 6(2): 15-24 (in Chinese)
- 835 Xu Z W, Lu H Y, Yi S W, Vandenberghe J, Mason J A, Zhou Y L, Wang X Y, 2015. Climate-driven changes to dune  
836 activity during the Last Glacial Maximum and deglaciation in the Mu Us dune field, north-central China. *Earth*  
837 *Planet Sci Lett*, 427: 149-159
- 838 Yang S, Jin, 2010. Isotopic records of oxygen and deuterium in ice wedges from Yituli'he, Northeast China and their  
839 paleoclimatic indications. *Sci China, Ser D: Earth Sci*, 54(D1): 119-126 (in Chinese)
- 840 Yang S, Cao X, Jin H, 2015. Validation of ice-wedge isotopes at Yituli'he, northeastern China as climate proxy. *Boreas*,  
841 44(3): 502-510
- 842 Yang X, Du S, Zhang F, 2006. Evolution of palaeoclimate in Hulunbeir Plateau since the Late Pleistocene. *J Nat Disast*,  
843 15(2): 157-159 (in Chinese)
- 844 Yang Y, Wang F, 1983. Pleistocene Glaciations and paleoclimate in Xizang (Tibet). *Quaternary Geology in Xizang*  
845 *(Tibet)*. Beijing: Science Press, pp. 91-99 (in Chinese)
- 846 Yao T, Shi Y, 1992. Changes of Holocene Climate recorded in the Dunde Ice-cores in the Qilian Mountains. Shi Y ed.,  
847 *Clim Environ in China during the Holocene Megathermal Period*. Beijing: Ocean Press, pp. 206-211 (in Chinese)
- 848 Yu K, Lu H, Lehmkuhl F, Nottebaum V, 2013. A preliminary quantitative paleoclimate reconstruction of the dune fields  
849 of North China during the Last Glacial Maximum and Holocene Optimum. *Quat Sci*, 33(2): 293-302 (in Chinese)
- 850 Zhang H, 2009. A review of the study of environmental changes and extinction of the *Mamuthus-Colelodonta* Fauna  
851 during the Middle-Late Pleistocene in NE China. *Adv Earth Sci*, 24: 49-60 (in Chinese)
- 852 Zhang W, 1983. Characteristics of sands wedges along the Qinghai-Xizang (Tibet) Highway and their formation time.  
853 Lanzhou Institute of Glaciology and Cryopedology (Geocryology), Chinese Academy of Sciences edited,  
854 *Proceedings of the 2<sup>nd</sup> Chinese Conference on Geocryology*. Lanzhou: Gansu People's Press, pp. 52-57 (in Chinese)

- 855 Zhao L, Jin H J, Li C C, Cui Z J, Chang X L, Marchenko S S, Vandenberghe J, Zhang T J, Luo D L, Guo D X, Liu G N  
856 and Yi C L, 2013. The extent of permafrost in China during the local Last Glacial Maximum (LLGM). *Boreas*,  
857 43(3): 688-698. doi: 10.1111/bor.12049
- 858 Zheng B, 1990. The glacier, environment and its changes since the Last Glaciation in West China. *Quat Sci*, 10(2): 101-  
859 110 (in Chinese)
- 860 Zheng Z, Yuan B Y, Petit-Maire N N, 1998. Paleoenvironments in China during the Last Glaciation Maximum and the  
861 Holocene Optimum. *Episodes*, 21: 152-158
- 862 Zhou T, 2007. *Evolution of permafrost boundaries in China since the Penultimate Glaciation*. A Master's Thesis of  
863 Lanzhou University, 1-59 (in Chinese)
- 864 Zhou T, Pan B, Liu X, Su H, Hu Z, 2008. The discovery of ice-wedge casts in Erdos: Rebuilding the permafrost  
865 boundary during the Penultimate Glaciation in China. *Quat Sci*, 30(1): 108-112 (in Chinese)
- 866 Zhou Y, 1965. Permafrost along the Qinghai-Xizang (Tibet) Highway. *Collective Papers on Permafrost Expeditions*  
867 *along the Qinghai-Xizang (Tibet) Highway*. Beijing: Science Press, pp. 1-10 (in Chinese)
- 868 Zhou Y, Qiu G, Guo D, 1991. Quaternary permafrost in China. *Quat Sci Rev*, 10: 511-517
- 869 Zhou Y, Qiu G, Cheng G, Guo D, Li S, 2000. *Geocryology in China*. Beijing: Science Press, pp. 366-388 (in Chinese)
- 870 Zhu K, 1972. Preliminary discussion on climate evolution in China during the last 5,000 years. *Act Archaeol Sin*, (1):  
871 15-38 (in Chinese)